Characterization of the reception environment of GNSS signals using a texture and color based adaptive segmentation technique

Andrea Cohen, Cyril Meurie, Yassine Ruichek, Juliette Marais

▶ **To cite this version:**

Andrea Cohen, Cyril Meurie, Yassine Ruichek, Juliette Marais. Characterization of the reception environment of GNSS signals using a texture and color based adaptive segmentation technique. 2010 IEEE Intelligent Vehicles Symposium (IV), Jun 2010, La Jolla, United States. pp.275-280, 10.1109/IVS.2010.5548018 . hal-04757929

HAL Id: hal-04757929
https://hal.science/hal-04757929v1

Submitted on 29 Oct 2024

HAL is a multi-disciplinary open access archive for the deposit and dissemination of scientific research documents, whether they are published or not. The documents may come from teaching and research institutions in France or abroad, or from public or private research centers.

L'archive ouverte pluridisciplinaire **HAL**, est destinée au dépôt et à la diffusion de documents scientifiques de niveau recherche, publiés ou non, émanant des établissements d'enseignement et de recherche français ou étrangers, des laboratoires publics ou privés.

Characterization of the reception environment of GNSS signals using a texture and color based adaptive segmentation technique

Andrea Cohen and Cyril Meurie and Yassine Ruichek and Juliette Marais

***Abstract*— This paper is focused on the characterization of GNSS signals reception environment by estimating the percentage of visible sky. A new segmentation technique based on a color watershed using an adaptive combination of color and texture information is proposed. This information is represented by two morphological gradients, a classical color gradient and a texture gradient based on co-occurrence matrices. The segmented images are then used as input for a k-means classifier in order to determine the percentage of visible sky in fish-eye images. The obtained classification results are evaluated to demonstrate the effectiveness and the reliability of the proposed approach.**

I. INTRODUCTION

Positioning is the central function of most of the ITS or robotics mobile applications. This function often relies on the American GPS constellation which suffers, however, of inaccuracy or unavailability on constrained environments due to multipath or signals blocking. The GNSS (Global Navigation Satellite System) panorama will soon be completed by the modernization of Russian GLONASS, the new European Galileo, the Chinese COMPASS and other Satellite-Based Augmentation Systems (SBAS) that will enhance the global availability and enhance the performance. Still, in dense urban environments or other masked area, the number of satellites received will not solve the propagation difficulties. Different levels of work can be chosen to mitigate its impacts: from the antenna choice to the multisensor solution, and the new correlation techniques. The solution on which this paper is focused was inspired by land-mobile satellite (LMS) communication studies [1] and aims to detect the satellite state of reception of each signal versus time based on a video record of the surrounding environment. Signals are usually classified in the literature into three states: blocked (no signal received), shadowed (signal attenuated, mainly by vegetation), and direct or clear. In positioning systems where the main objective of the signal reception is the propagation time estimation, the following three states have been defined: blocked; shadowed or alternate path represents the case where the signal is received after reflections without any direct ray; direct.

In terms of sensor behavior, we can consider that the direct state is the nominal mode, the alternate, a degraded mode and blocked, a failure. The consequence of the degraded mode is inaccuracy of the positioning solution. In order to limit it, some authors choose to exclude the concerned satellites from the positioning computation [2] which can result in more unavailability. Another approach consists in considering the error bias included by the degraded signal in a new filtering process in order to reduce the error impact without increasing unavailability [3]. In these works, one seek to estimate the state of the signals, and consequently the quality of the measure, so as to ensure both precision and availability, as described in [4].

The present paper will focus on the method used to detect the satellite state of reception that uses a video recording of the environment surrounding the GPS antenna. The antenna is omni-directional and satellites with an elevation under 10 degrees are not taken into account. The camera used is a fish-eye camera which has a field of vision of 180 degrees which covers the reception field of the antenna. This system has been developed for the first version of the PREDISSAT tool [5] and has inspired other developments with infra-red cameras [2]. The goal of this paper is to benefit from new image processing developments in order to enhance satellite state reception and masking elements. The main idea is to detect the portion of visible sky. This, as well as the information concerning satellite position, which is known since we use a GNSS constellation, will allow us to place the satellites on the image in order to know the state of their signals. The aim of this paper consists in determining the percentage of visible sky. For that, the process starts by segmenting the image into regions of interest according to a given criteria. Afterwards, the obtained regions have to be classified into at least two classes, which correspond to the sky and the rest of the image (vegetation, buildings, ...). Many segmentation methods are proposed in the literature. Most of them can be grouped into two categories: edges and/or regions based segmentation. These methods are generally developed considering specific applications. Therefore, there is no method that can be successfully applied for any application. In the context of our application, images present two important informations: color and texture. It is hence useful to use a segmentation method based on these informations. Angulo [6] proposes a segmentation method combining color and texture informations. However, this method involves many parameters, which are difficult to adjust according to the considered application. Based on the texture gradient proposed by Angulo [6], we have proposed in previous works a new segmentation method based on a

A. Cohen, C. Meurie and Y. Ruichek are with the Systems and Transportation Laboratory, University of Technology of Belfort-Montbeliard, 13 rue Ernest Thierry Mieg, 90010 Belfort Cedex, France; {andrea.cohen, cyril.meurie, yassine ruichek }@utbm.fr

J. Marais is with the Univ Lille Nord de France, Lille, France - INRETS, LEOST, Villeneuve d'Ascq, France, 20 rue Elisée Reclus, 59650 Villeneuve d'Ascq, France juliette.marais@inrets.fr

This research work is developped in the framework of the ViLoc project, supported by the Regional Council of Franche-Comté (France).

non-parametric and adaptive combination of color and texture information. Many papers can be found in the literature that use co-occurrence matrices to extract the texture features of an image [7] [8] [9] [10]. In this paper, we develop a new texture gradient based on these co-occurrence matrices and a new segmentation technique using an original and adaptive combination (considering local image content) to take into account color and texture gradients.

The paper is organized as follows. Section 2 presents the morphological texture and color gradients definition. Section 3 describes the structural gradient process and the proposed strategy to combine texture and color gradients. The segmentation by color watershed algorithm is explained in section 4. Before concluding, experimental results with real images are presented in section 5.

II. Morphological texture and color gradients definition

The process to obtain a texture gradient will be presented in three parts: 1/ Co-occurrence matrices; 2/ Local analysis; 3/ Morphological texture gradient computation.

A. Co-occurrence matrices

A co-occurrence matrix is essentially a two-dimensional histogram of the number of times that pairs of intensity values occur in a given spatial relationship (or translation) [9]. Mathematically, a co-occurrence matrix C is defined over an gray scale image g, parameterized by a translation $\vec{t}$, as:

$$C_{\vec{t}}(i,j) = card\{(x, x+\vec{t}) \in D : g(x) = i, g(x+\vec{t}) = j\} \quad (1)$$

where $g(x)$ is the gray level for the pixel x; i and j are gray levels, and D is the domain of the image.

A co-occurrence matrix describes an image by looking at the relation between neighbor pixels and not each pixel separately. Texture, on the other hand, is a phenomenon associated to a neighborhood of pixels and not to an individual pixel, hence, co-occurrence matrices can be used as a tool for texture description. Nevertheless, the success of this tool highly depends on the spatial relationship (translation vector) chosen.

There are several characteristic features of co-occurrence matrices that can be used for textural description. These features summarize the content of the matrices. There is a total of 13 of these features that have been presented by Haralick et al [8]. Only two of them will be presented and used in this paper: the angular second moment (ASM) and the contrast (c).

$$ASM_{\vec{t}} = \sum_{i=0}^{G-1} \sum_{j=0}^{G-1} C_{\vec{t}}^2(i,j) \quad (2)$$

$$c_{\vec{t}} = \sum_{i=0}^{G-1} \sum_{j=0}^{G-1} (i-j)^2 C_{\vec{t}}(i,j) \quad (3)$$

The ASM is a measure of the homogeneity of the texture for the given spatial relationship. Its value is high when the same couple of pixels is found repeatedly throughout the image. This results in a matrix that has few entries of large magnitude. The contrast feature is a measure of the amount of local variation of the texture according to the spatial relationship. It is high when the matrix presents large terms far away from the diagonal. This means that pixels that are neighbors in terms of vector $\vec{t}$ have very different intensity values.

B. Local Analysis

As presented on the preceding section, co-occurrence matrices can be used to obtain texture features. Nevertheless, they are computed globally for the entire image, while the expectation is to obtain more than one texture per image. Indeed, the classification should be able to be applied for each pixel of the image f. To solve this problem, a co-occurrence matrix is computed locally for each pixel. This can be done by calculating C on a window centered on each pixel x. In this way, both measures (ASM and contrast) can be computed for each pixel of the image. It is defined as the local ASM image associated to $\vec{t}$ the image that groups the ASM measures associated to the translation $\vec{t}$ of each pixel of the image. The same concept can be applied to the contrast, resulting in a local contrast image associated to $\vec{t}$. In a $\vec{t}$-oriented local ASM image (resp. contrast image), pixels associated to a texture that's homogeneous in the direction and size of $\vec{t}$ (or that presents a lot of contrast for the contrast image) are affected with a high value. The images obtained by this procedure are then normalized.

C. Morphological texture gradient definition

A morphological texture gradient is defined in terms of the concept of local ASM and contrast images presented previously. In general, a morphological gradient is defined, for a gray-scale image g, as the residue of dilatation and erosion (computed usually with a structuring element of size 1). In this paper, the structuring element used is a disc with radius 1.

$$Q(g(x)) = \delta_\beta(g(x)) - \epsilon_\beta(g(x)) \quad (4)$$

The $\vec{t}$-oriented local ASM images computed for each color plane of the image f in RGB color space will be referred to as $ASM_{\vec{t}}^R$, $ASM_{\vec{t}}^G$, $ASM_{\vec{t}}^B$. The $\vec{t}$-oriented local contrast images computed for each color plane of the image f in RGB color space will be referred to as $c_{\vec{t}}^R$,$c_{\vec{t}}^G$ and $c_{\vec{t}}^B$. Two texture gradients will be defined for the image, one in reference to the morphological gradient of each $ASM_{\vec{t}}$, and another one in reference to the morphological gradient of each $c_{\vec{t}}$.

$$Q_{ASM}(f(x)) = \bigvee_{t \in T} \bigvee_{R,G,B} [Q(ASM_{\vec{t}}(x))] \quad (5)$$

$$Q_c(f(x)) = \bigvee_{t \in T} \bigvee_{R,G,B} [Q(c_{\vec{t}}(x))] \quad (6)$$

where T is a set of translation vectors of different sizes and orientations and $\bigvee$ represents the supremum operator.

D. Morphological color gradient definition

The classical definition of the morphological gradient for a gray scale image g is given by: $\nabla g = \delta(g) - \epsilon(g)$. The extension of gray scale image algorithms to color or vector valued images is not simple since there is no natural ordering on a set of color vectors, and more generally of multivariate data. According to Barnett [11], there are several possible types of multidimensional vector ordering: marginal ordering, reduced ordering, partial ordering and conditional ordering, etc. In this paper, the conditional ordering is considered.

Let $x_1, x_2, \cdots, x_n$ denote a set of n p-dimensional vectors: $x_i = \{x_{1(i)}, x_{2(i)}, \cdots, x_{p(i)}\}, x_i \in R^p$. In the conditional (also called lexicographic) ordering, the vectors are ordered according to a hierarchical order of the component (Red then Green then Blue in RGB color space). For two vectors x_i and x_j, one has:

$$x_i \leq x_j \begin{cases} x_{1(i)} < x_{1(j)} \text{ or} \\ x_{1(i)} = x_{1(j)} \text{ and } x_{2(i)} < x_{2(j)} \text{ or} \cdots \\ x_{1(i)} = x_{1(j)} \text{ and } x_{2(i)} = x_{2(j)} \cdots \ x_{p(i)} < x_{p(j)} \end{cases}$$

If f is a color image, $\delta(f)$ and $\epsilon(f)$ are color vectors and the classical morphological color gradient ∇f is given by: $\nabla f = \delta(f) - \epsilon(f)$.

III. Structural gradient definition

In order to achieve a robust and reliable segmentation, it is very useful to use both texture and color information. The main idea is to produce a structural gradient by combining the texture and color gradients. The problem is the fact that the color gradient is a color image while the texture gradient is a gray level one. To solve this problem, the proposed method starts by decomposing the color gradient image Q_{col} into its three components, which are Q^R_{col}, Q^G_{col} and Q^B_{col}. In the next step, each component of the color gradient image is combined with the texture gradient image Q_{tex} (which can be $Q_{ASM}(f(x))$ or $Q_c(f(x))$). This operation produces three gray levels images Q^R, Q^G and Q^B:

$$\begin{cases} Q^R = Q^R_{col} \otimes Q_{tex} \\ Q^G = Q^G_{col} \otimes Q_{tex} \\ Q^B = Q^B_{col} \otimes Q_{tex} \end{cases} \tag{7}$$

where the operator $\otimes$ represents the combination of two gray-level images which will be described on the following sections.

Q^R, Q^G and Q^B can be interpreted as the color components of a new color image, which is proposed to define the needed structural gradient. In other words, the structural gradient Q is defined as a color image with Q^R as the red component, Q^G as the green component, and Q^B as the blue component. This combination approach is suitable because, not only color information is preserved, but also the texture information is added to each color component. Indeed, texture, which is not a color phenomenon, is supposed to affect all colors equally. To combine a component of the color gradient image q and the texture gradient image r, three techniques are used: fixed combination, adaptive combination, supremum combination. Let h be the output of the combination process (represented by $\otimes$ on the preceding equation), which is applied for each pixel.

A. Fixed combination

The fixed combination is defined as a barycentric sum of the color gradient image and the texture gradient image. It uses a global weighting coefficient referred to as α:

$$h(p) = \alpha q(p) + (1 - \alpha) \times r(p) \tag{8}$$

where α is a constant coefficient taking its value in $[0; 1]$. The combination technique is not generally suitable, due to the coefficient α, which is constant for the entire image. Indeed, one may need to give priority to color or texture according to their importance in the different zones of the image. This technique requires manual adjustment of the coefficient α according to the content of the image.

B. Adaptive combination

The proposed adaptive combination strategy uses a modular combination of texture and color gradients according to the content of the image. It implies two advantages: First, it gives priority to the most important information (the color or the texture) for a given pixel. Second, it constitutes an automatic method, which can perform for all types of images. The adaptive combination is expressed as follows:

$$h(p) = \alpha_p q(p) + (1 - \alpha_p) \times r(p) \tag{9}$$

α_p is a coefficient taking its value in $[0; 1]$. It is calculated for each pixel p in order to give a high weight to the image that provides the most important information for the pixel. In other words, α_p is high if the information is more important for q than for r (and vice-versa). It is computed as follows:

$$\alpha_p = \frac{q(p)}{q(p) + r(p)} \tag{10}$$

C. Supremum combination

Using the same principle as in the adaptive strategy, the supremum combination is sensibly different. There is actually no combination at pixel level. Indeed, for a given pixel, the modular gradient is either a copy of the color gradient or the texture gradient depending on which one of them provides the biggest amount of information (the supremum). This combination has the same advantages as the adaptive one.

$$h(p) = \begin{cases} q(p), & \text{si } q(p) \geq r(p) \\ r(p), & \text{si } r(p) > q(p) \end{cases}$$

IV. Segmentation by color watershed

The watershed algorithm is one of the principal mathematical morphology image processing operations [12], [13]. It permits to segment an image into homogeneous regions from a seeds image (markers) and a potential image (gradient). Image segmentation based on the watershed algorithm has proved to be a powerful segmentation tool

but, unfortunately, when directly applied to an image, this algorithm presents a strong over segmentation. One way to suppress this over segmentation is to use a non-parametric hierarchy of watershed, also known as the waterfall algorithm [14]. Several authors propose different types of gradients including several ordering of color vectors [15], [16]. But in the context of our application, the processing time of this approach would be too important. That is why, we prefer to define an specific image of seeds positioned experimentally and adapted to our application (few germes located on the borders of the image, since objects tend to be found on this region of the image due to fish-eye lens distortion). The watershed algorithm makes regions grow from the initial seeds using the priority given by the potential image (structural gradient based on color and texture informations).

V. Experimental Results

A. Evaluation method

In this section, the discussion is focused on the classification results, which are based on the segmentation results presented in the previous section. The classification process is performed using the K-means algorithm. The goal is to classify the image regions into two classes: sky region and not-sky region. For the evaluation, a classification reference image is created. For each result, four measurements are computed: the percentage of pixels that actually make part of the sky region in the classification reference image, the percentage of pixels classified as sky but do not make part of the sky region, the percentage of pixels classified as not-sky and are effectively in the no-sky region. The fourth measurement, which is computed as the sum of the first and third measurements, can be viewed as the percentage of pixels that are correctly classified. For an easier interpretation of the results, the symbols $C = \alpha$ and $T = 1-\alpha$ will be used when making references to the fixed combination method.

B. Observations

Figure 2 (lines 2-6) presents the segmentation results obtained for the fixed combination method (with different coefficients) and the adaptive and supremum methods. The texture gradient used for these tests is the contrast gradient computed for the best vector set (see number 4 in [17] for more details). After a visual evaluation of the different segmentation results, several observations can be made. First of all, the segmentation results obtained by the use of the co-occurence based texture gradient alone are not as bad as those obtained with a morphological texture gradient presented by Angulo (and tested in previous works [18]). On the other hand, the fixed method presents both good and bad results depending on the image and on the coefficients used. For example, a coefficient of 0.2 color/0.8 texture works well enough for images 4 to 8, specially for image 7 in which a small region at the top part representing a building is well detected. However, for images 1 and 2 both vegetation and sky regions are over-segmented. The same conclusion can be made for a 0.5/0.5 combination. It presents the most accurate segmentation for images 5 and 3, but it works very badly for image 1 since it detects a region that doesn't exist right in the middle of the sky and it over-segments the sky region in image 2. For a coefficient of 0.7 color/0.3 texture the same inconsistencies can be found. For example, the sky region is divided into two onestwo for image 2 and the house in image 7 is not well segmented. There is also a bad segmentation of the sky in image 6. These results clearly illustrate that there is no way of choosing a fixed coefficient that works for all images, since those that work very well for one image can lead to disastrous results for other ones.

On the other hand, both the adaptive and supremum combination methods present acceptable segmentations for all images, and, in general, less over-segmentation. In addition, they present the best segmentation for some of the images, such as images 7 and 8. These demonstrates that by adapting the coefficient to the local image content we obtain a method that's consistent and that performs well for all images.

Figure 1 (left and middle) represents the performance of the fixed combination method (for coefficients 0, 0.2, 0.5, 0.7 and 1), the adaptive and supremum methods. The first graph (left) shows the results for the contrast gradient while the second one (middle) shows the results of the ASM gradient. The evaluation is achieved by computing an average percentage of well classified pixels over all tested images (represented on the Y axis) for different offset vectors sets which represent the X axis. Presenting higher good classification rates for all sets of vectors and for all combination methods, only the contrast gradient will be analyzed in this section.

Taking a closer look at the first graph presented in figure 1, one can see that the highest rates are achieved by the adaptive method, the supremum method and the fixed method with a weighing coefficient of 0.7 color/0.3 texture. However, for the supremum method, there is hardly any variation on the rates obtained for different vector sets (it varies between 93.6% and 93.7%) while the fixed method (for 0.7 color/0.3 texture.) gets a rate between 90.3% and 93.79% depending on the chosen vector set. This is clearly an advantage for the supremum method since the choice of a set of vectors is no longer a problem, being possible to chose the smallest set of vectors which results in a faster performance. Furthermore, the supremum method does not require any parameters while the fixed method requires a careful choice of the weighing coefficient. However, the parameters adjustment is never optimal and then inconsistencies can still occur.

Classification results for all the tested combination methods (taking into account only the contrast gradient) for the best vector set (see number 4 in [17] for more details) are presented in figure 2 (lines 7-11). This figure represents the percentage of well classified pixels (Y axis) for each one of the 8 images of the database (X axis). Each curve represents a combination method. For images 1, 3 and 4, using the color alone presents the best results, while for images 2 and 5 the best results correspond to a coefficient of 0.7 color/0.3 texture. For image 8, the coefficient of 0.2 color/0.8 texture works best. It could be assumed that color alone, and a coefficient of 0.7 color/0.3 texture are the best

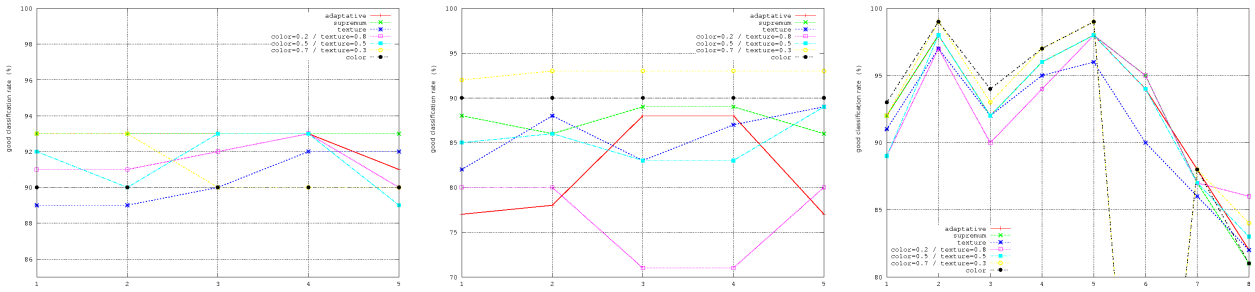

Fig. 1. Average classification results with different combinations for all sets of vectors for ASM (left) and contrast (middle) gradients, and classification results with different combinations for contrast gradient (with vector set number 4) and for each image of the database (right).

TABLE I

COMPARISON BETWEEN DIFFERENT METHODS

method	k-means	approach [18]	proposed approach
adaptatif	42,25	**95,6**	93,9
supremum	42,25	91,7	**93,7**
C=0/T=1	42,25	84,7	92,6
C=0.2/T=0.8	42,25	93,4	93,0
C=0.5/T=0.5	42,25	94,4	93,1
C=0.7/T=0.3	42,25	94,8	93,9
C=1/T=0	42,25	90,2	90,2

weighing coefficients for this set of vectors and for this application. Nevertheless, both of them present unacceptable results for image 8. This is a clear example of the major difficulty that represents parameters setting. On the other hand, adaptive and supremum methods present the best results for images 6 and 7, and on the other images, they are always among the second and third best classifications, which means that they present acceptable results for all images without having the problem of parameters setting. These results are illustrated in figure 1 (right). We have compared our method to two other techniques: the firs one, presented on previous works [18], is similar to the one presented on this paper but uses a morphological texture gradient instead of a gradient based on cooccurrence matrices; the second method performs a classification by the k-means algorithm directly on the original images, meaning there is no pre-segmentation of the image. The comparison results are presented in Table I. Applied directly on the original image, the k-means algorithm presents very bad results, with an average classification rate of 42.3%. On the other hand, with the morphological gradient, the results are better for the adaptive method (95.6%), while the proposed method presents better results for the supremum method (93.7%), with the advantage of being faster in terms of computation time.

VI. CONCLUSION

A new segmentation method that combines both color and texture information is presented. This technique is used to extract the percentage of visible sky by means of the k-means algorithm. This information will allow the characterization of the environment of reception of GNSS signals. The first original contribution of this paper is the obtention of a morphological gradient based on co-occurrence matrices. The second contribution of the proposed technique is that it takes into account local image content by automatically computing the weighting coefficients for color and texture. This method provides very good results, compared with a method based on a fixed combination of color and texture information. The drawback of this last approach is that it requires a manual adjustment of the weighting coefficients which are global for all the pixels of the image, while the proposed method does not require any parameters setting. The classification results for the proposed approach are very satisfactory considering those obtained by the other methods. Compared to a simple classification with the k-means algorithm, the classification rate of the proposed method is 93.7 % (VS 42,25 %). Compared to previous works, the classification rate obtained is 93.7 % VS 91.7 %. Future works are in progress and concern the computation of the texture gradient in real time.

REFERENCES

[1] H.-P. Lin, R. Akturan, and W.-J. Vogel, "Satellite-pcs channel simulation in mobile user environments using photogrammetry and markov chains," *Wireless Networks*, vol. 3, pp. 299–308, 1997.

[2] J.-I. Meguro, T. Murata, J.-I. Takiguchi, Y. Amano, and T. Hashizume, "Gps multipath mitigation for urban area using omnidirectional infrared camera," *IEEE Trans. On Intelligent Transportation Systems*, vol. 10, no. 1, pp. 22–30, Mar. 2009.

[3] A. Rabaoui, N. Viandier, J. Marais, and E. Duflos, "Using dirichlet process mixtures for the modelling of gnss pseudorange errors in urban canyon," in *ION-GNSS*, Sept. 2009, pp. 22–25.

[4] D. F. Nahimana, J. Marais, and E. Duflos, "A jump markov system for modelling a realistic error model depending on satellite reception state in urban environment," in *ION GNSS*, 2007, p. 7.

[5] J. Marais, M. Berbineau, and M. Heddebaut, "Land mobile gnss, availability and multipath evaluation tool," *IEEE Trans. On Vehicular Technology*, vol. 54, no. 5, pp. 1697–1704, Sept. 2005.

[6] J. Angulo, "Gradients morphologiques de texture. application à la segmentation couleur+texture par lpe," in *COmpression et REprésentation des Siganux Audiovisuels*, Nov. 2006, pp. 42–47.

[7] P. Kruizinga and N. Petkov, "Nonlinear operator for oriented texture," *IEEE Transactions on image processing*, vol. 8, no. 10, pp. 1395–1407, Oct. 1999.

[8] R. M. Haralick, K. Shanmugan, and I. Dinstein, "Textural features for image classification," *IEEE Trans. On Systems, Man, and Cybernetics*, vol. 3, no. 6, pp. 610–621, Nov. 1973.

[9] S. W. Zucker and D. Terzopoulos, "Finding structure in co-occurrence matrices for texture analysis," *Computer Graphics and Image Processing*, vol. 12, pp. 286–308, 1980.

[10] A. Baraldi and F. Parmiggiani, "An investigation of the textural characteristics associated with gray level cooccurrence matrix statistical parameters," *IEEE Trans. On Geoscience and Remote Sensing*, vol. 33, no. 2, Mar. 1995.

Fig. 2. Segmented and classified images for different gradient combinations (top to bottom: initial images, segmented images (lines 2-6: with C=0.2/T=0.8; with C=0.5/T=0.5; with C=0.8/T=0.2; with adaptive combination, with supremum combination), classified images (lines 7-11: with the same combinations)).

[11] V. Barnett, "The ordering of multivariate data," *Journal of the royal society of statistics*, vol. A139, no. 3, pp. 318–355, 1976.

[12] L. Vincent and P. Soille, "Watersheds in digital spaces : an efficient algorithm based on immersions simulations," *IEEE Trans. On Pattern Analysis and Machine Intelligence (PAMI)*, vol. 13, no. 16, pp. 583–598, 1991.

[13] L. Shafarenko, M. Petrou, and J. Kittler, "Automatic watershed segmentation of randomly textured color images," *IEEE Trans. On Image Processing*, vol. 6, no. 11, pp. 1530–1543, 1997.

[14] S. Beucher, "Watershed, hierarchical segmentation and waterfall algorithm," *Mathematical morphology and its applications to image ans signal processing*, pp. 69–76, 1994.

[15] J. Angulo and J. Serra, "Color segmentation by ordered mergings," in *International Conference on Image Processing (ICIP)*, vol. 2, 2003, pp. 125–128.

[16] O. Lezoray, C. Meurie, and A. Elmoataz, "A graph approach to color mathematical morphology," in *IEEE Symposium on Signal Processing and Information Technology (ISSPIT)*, 2005, pp. 856–861.

[17] C. Meurie, A. Cohen, and Y. Ruichek, "An efficient combination of texture and color information for watershed segmentation." in *International Conference on Image and Signal Processing (ICISP), LNCS 6134*, 2010, pp. 147–156.

[18] A. Cohen, C. Meurie, Y. Ruichek, J. Marais, and A. Flancquart, "Quantification of gnss signals accuracy: an image segmentation method for estimating the percentage of sky." in *IEEE International Conference on Vehicular Electronics and Safety*, Nov. 2009, pp. 40–45.